J Mol Model (2015) 21: 8
DOI 10.1007/s00894-014-2525-9

ORIGINAL PAPER

Targeting a cluster of arginine residues of neuraminidase to avoid oseltamivir resistance in influenza A (H1N1): a theoretical study

L. Ramírez-Salinas Gema · L. E. Tolentino-Lopez · F. Martínez-Ramos · I. Padilla-Martínez · J. García-Machorro · J. Correa-Basurto

Received: 9 January 2014 / Accepted: 10 November 2014 / Published online: 22 January 2015

Abstract Following the influenza A (H1N1) pandemic in Mexico and around the world in 2009, the numbers of oseltamivir-resistant clinical cases have increased through a mechanism that remains unclear. In this work, we focus on studying the mutated NA structures ADA71175 (GenBank) and 3CKZ (PDB ID). Recently crystallized NA (PDB ID: 3NSS) was used as a wild-type structure and template to construct the three-dimensional (3D) structure of ADA71175. Then, the NA mutants and 3NSS natives as well as their refined monomer structures as determined through MD simulations (snapshots at 50 ns) were used as models to perform a docking study using a set of aryl-oseltamivir derivatives. These aryl-oseltamivir derivatives have better recognition properties than oseltamivir because of cation–π interactions with a cluster of Arg residues (118, 292, and 371) at the binding site. This cluster of Arg residues represents a potential binding site for aryl-oseltamivir derivatives that are potentially new NA inhibitors.

Keywords Oseltamivir · Neuraminidase · Mutation H275Y · π-cation interactions · Resistance

L. R.-S. Gema · L. E. Tolentino-Lopez · J. Correa-Basurto (✉)
Laboratorio de Modelado Molecular y Diseño de Fármacos (Laboratory of Molecular Modeling and Drug Design), Sección de Estudios de Posgrado e Investigación, Escuela Superior de Medicina, Instituto Politécnico Nacional, Plan de San Luis y Díaz Mirón, 11340 México City, Mexico
e-mail: corrjose@gmail.com

L. E. Tolentino-Lopez · F. Martínez-Ramos
Laboratorio de Investigación, Departamento de Química Inorgánica, Escuela Nacional de Ciencias Biológicas, Instituto Politécnico Nacional, Prolongación de Carpio y Plan de Ayala, 11340 México, DF, Mexico

I. Padilla-Martínez
Laboratorio de Investigación de Química Supramolecular, Unidad Profesional Interdisciplinaria de Biotecnología, Instituto Politécnico Nacional, Av. Acueducto s/n., Barrio La Laguna, col. Ticomán, C.P. 07340 México, DF, Mexico

J. García-Machorro
Laboratorio de Medicina de Conservación, Sección de Estudios de Posgrado e Investigación, Escuela Superior de Medicina, Instituto Politécnico Nacional, Plan de San Luis y Díaz Mirón, 11340 México, DF, Mexico

Introduction

It is known that the binding modes of ligands on protein-binding sites [1] are determined by their chemical and geometrical properties. Several factors influence the formation of a protein pocket that allows the ligand to become coupled. However, the shape of the binding site can be modified by conformational motions induced by several factors, such as membrane voltage [2] and water molecules [3], among others. The amino-acid mutations at the protein-binding site are the most common factors that induce shape changes that affect ligand recognition [4]. RNA virus tends to mutate frequently; one such influenza virus, AH1N1, possesses a protein known as neuraminidase (NA), which is a sialidase that catalyzes the removal of sialic acid residues from the glycoconjugates to facilitate the release of viruses from infected cells and prevent self-aggregation. This process is mediated by the NA active site that hydrolyzes the terminal sialic acid of the glycosylated receptor associated with hemagglutinin (HA) [5]. It is well known that NA from influenza A (H1N1) can possess oseltamivir resistance through the presence of mutations such as

H275Y, [6, 7] N294S [8], and I222R [9], whereas other residues are highly conserved in terms of oseltamivir recognition (R118, D151, R152, R224, E277, R292, R371, and Y407) [10]. After the H1N1 strain pandemic occurred in 2009, a substantial amount of experimental data became available concerning the oseltamivir resistance caused by NA mutations [11]. However, there are not clearly relationship between the H275Y mutan and the oseltamivir resitance [12]. Recently, a sequence analysis report has been released that does not reveal molecular markers for drug resistance (e.g., H275Y) that could explain the NA inhibitor resistance; instead, it reveals mutations outside of the NA active site, as well as other associated factors [13]. During the 2009 pandemic of this strain in Mexico, research groups focused on performing diagnostics based on PCR studies to identify several mutations that were seldom found at binding sites [14]; however, NA mutations outside the binding sites were found [15, 16]. The FDA permits the use of peramivir to treat patients who are resistant to oseltamivir [17]. However, some NA mutations affect the antiviral activity of peramivir [18]. Recently, NA resistance to oseltamivir and peramivir—attributed to H275Y and N294S mutants—has been reported, although both viruses remain susceptible to zanamivir [19]. In this context, Shie and colleagues have noted the importance of this cluster of Arg to zanamivir (phosphonate) derivatives; the high affinity of phosphonate derivatives can be partly attributed to the strong electrostatic interactions of their phosphonate groups with the cluster of Arg residues at the active site of NA [20], as in the case of the interaction of the carboxylate group of oseltamivir with clusters of Arg, or the effects of cation–π interactions on protein folding, structural stability, specificity, and molecular recognition, as in the case of lipocalin [21].

In this study, the Arg clusters (118, 292, and 371) of NA mutants (GenBank: ADA71175 and PDB ID: 3CKZ) and wild-type NA (PDB ID: 3NSS) in their native forms and in snapshot structures obtained from MD simulations (NA monomers) were used in docking studies to explore the possibility of avoiding oseltamivir resistance.

Methods

Sequence selection and alignment analysis

We obtained protein sequences from the NCBI (http://www.ncbi.nlm.nih.gov/protein) database (GenBank: ADA71175), which contains the NA mutants of interest (H275Y and other mutations outside the binding site [15]). In addition, we obtained the crystal structure 3CKZ (which contains the H275Y mutation) and the NA wild-type crystal structure (PDB code: 3NSS) to permit docking into the native structures and the structures obtained through MD simulations (50 ns).

Homology modeling

We constructed the NA dimer using the 3D model of the sequence ADA71175 (aa 82–470) by applying homology modeling using Modeller 9.10 and the 3NSS structure, which is 84 % identical to the structure of interest, as a model. The dimeric ADA71175 was quality checked using the ERRAT and RAMPAGE servers.

Ligand construction and optimization

Oseltamivir and its derivatives were constructed using the ChemBioDraw v.12.0 (http://www.cambridgesoft.com) software package, and geometric optimization was initially performed employing the program HYPERCHEM v.7.0 (Hypercube, USA, http://www.hyper.com) in the framework of molecular mechanics. The coordinates of the minimum geometries of the aryl-oseltamivir derivatives were obtained at the B3LYP/6-31* level of theory using the Gaussian 98 program [22].

Docking procedure

Docking simulations were performed using AutoDock 4.0.1 [23]. The ligands were prepared by adding all possible rotatable bonds, torsional degrees of freedom, Gasteiger–Marsili empirical atomic partial charges, and merged nonpolar hydrogens of the ligands using AutoDockTools 1.5.4, which is included in the AutoDock program [23]. The Kollman charges for all atoms of the investigated NA structures (natives and snapshots at 50 ns retrieved from the MD simulations) were assigned using AutoDockTools 1.5.4. Oseltamivir and its derivatives were docked using a rectangular grid box of size 68×60×60 Å that covered the active site, with the grid points separated by 0.375 Å on the NA tested using the AutoDock 4.0.1 software package by applying a hybrid Lamarckian genetic algorithm with an initial population of 100 randomly placed individuals and a maximum number of energy evaluations of 1×10^7. The resulting docked orientations were clustered together with root mean square deviations (RMSD) of ≤0.5 Å.

The lowest free-energy values of the protein–ligand complexes of each docking simulation of oseltamivir and its derivatives that were returned by AutoDock 4.0.1 were used for further analysis. The remaining parameters remained at their default settings. All ligand–enzyme complexes were visualized using VMD v. 1.9.1 [24] and the LIGPLOT program.

Results and discussion

There have been several reports concerning protein mutations at the binding site that frequently occur in certain proteins, such as β-lactamases [25]. However, the pocket surfaces or shapes are modified because of extraconformational changes, which can lead to either open or closed dynamics of structural components such as loops or domains [26]. Considering the structural factors that affect the binding poses and affinity values, in this study, we investigated two mutant and wild-type NA structures because it is known that NA mutants suffer conformational changes [16]. To begin, we performed docking studies to explore the native structures (Fig. 1), and then each protein (as a monomer) was subjected to MD simulations to induce certain structural changes that affected the binding-site recognition due to the lack of other monomers. These structural analyses were performed with the intent of explaining the behavior of the NA mutants and demonstrating that the ligands would reach the NA site despite the structural changes induced in the MD simulations. This approach was taken because the number of NA mutants associated with oseltamivir resistance is lower than the number observed in clinical cases [15]. For example, in 2011, Meijer et al. [27] reported that, among 1100 patients infected with H1N1, only 19 exhibited oseltamivir-resistant viruses harboring the H275Y mutation in the NA [27]. The estimated rate of resistance was 0.32–1 % in the adults [28, 29] who constituted the population most frequently affected during the 2009 pandemic [29]. This finding suggests that the resistance of the viruses could not have been attributable only to oseltamivir use [30].

In addition, our research group used our docking studies to demonstrate that the H275Y mutation decreases the affinity of oseltamivir (data not shown) but that the binding pose is maintained, as reported in [8]. Furthermore, we selected NA sequences that contained the H275Y mutation (see Fig. 2) plus a set of mutations outside the binding site; we then constructed the 3D structural model via homology modeling. Docking studies were performed on both the native NA and NA monomer structures retrieved from the MD simulations. Figure 3 illustrates the time evolution of the root-mean-square deviation (RMSD) of the frames with respect to the initial crystal structure during the last 90 ns of the MD simulations. The RMSD values with respect to the starting structure were calculated for all backbone Cα atoms of the entire enzyme. The plots of the evolution of the RMSD values throughout the simulation time are provided in Fig. 3 for the cases of 3NSS (black line), 3CKZ (gray line), and ADA71175 (red line). The lines represent the RMSD values of the backbone Cα atoms of the entire protein throughout the MD simulation time.

Fig. 1a–f Oseltamivir docked on **a** ADA71175-45, **b** 3NSS, and **c** 3CKZ, and **45** docked on **d** ADA71175, **e** 3NSS-osetamivir, and **f** 3CKZ using the native structures

It is clear from Fig. 3 that the black/red lines dynamic convergence was almost achieved by approximately 65 ns in both the ADA71175 and 3CKZ systems. The gray lines rapidly attained dynamic convergence with an RMSD of approximately 2.5–3.5 Å without any obvious converging trend within 70 ns, whereas the black/red lines fluctuated strongly between 4 and 5 Å.

However, because the 3D models that were obtained maintained the backbone of the template despite the presence of several structural differences from it, we performed MD simulations for 90 ns to refine the 3D models, using an approach similar to that already used by other authors [31]. The MD simulations demonstrated, based on the RMSD values, that the three investigated proteins reached convergence (Fig. 3), as reported elsewhere for NA subjected to MD simulations, which reached equilibration at 10 ns [32]. In addition, the MD simulations provided evidence that differences in the residues of the proteins reflect significant structural changes at the binding sites (Fig. 4). These findings are in agreement with other results recently reported by our research group [15], because the proteins were used as NA monomers to displace certain structural components without affecting the binding-site surfaces. Visual analysis of the oseltamivir binding sites in the target proteins—3NSS, 3CKZ, and ADA71175—revealed differences in the shapes of the active site of NA (Fig. 3a). Visualizer programs are available that can present the molecular surface of the protein with a large amount of structural detail, thereby allowing one to visualize many structural details associated with the similarities and differences in the protein surfaces; these programs have been used to explore other NAs and illustrate the differences among NA subtypes [33]. As

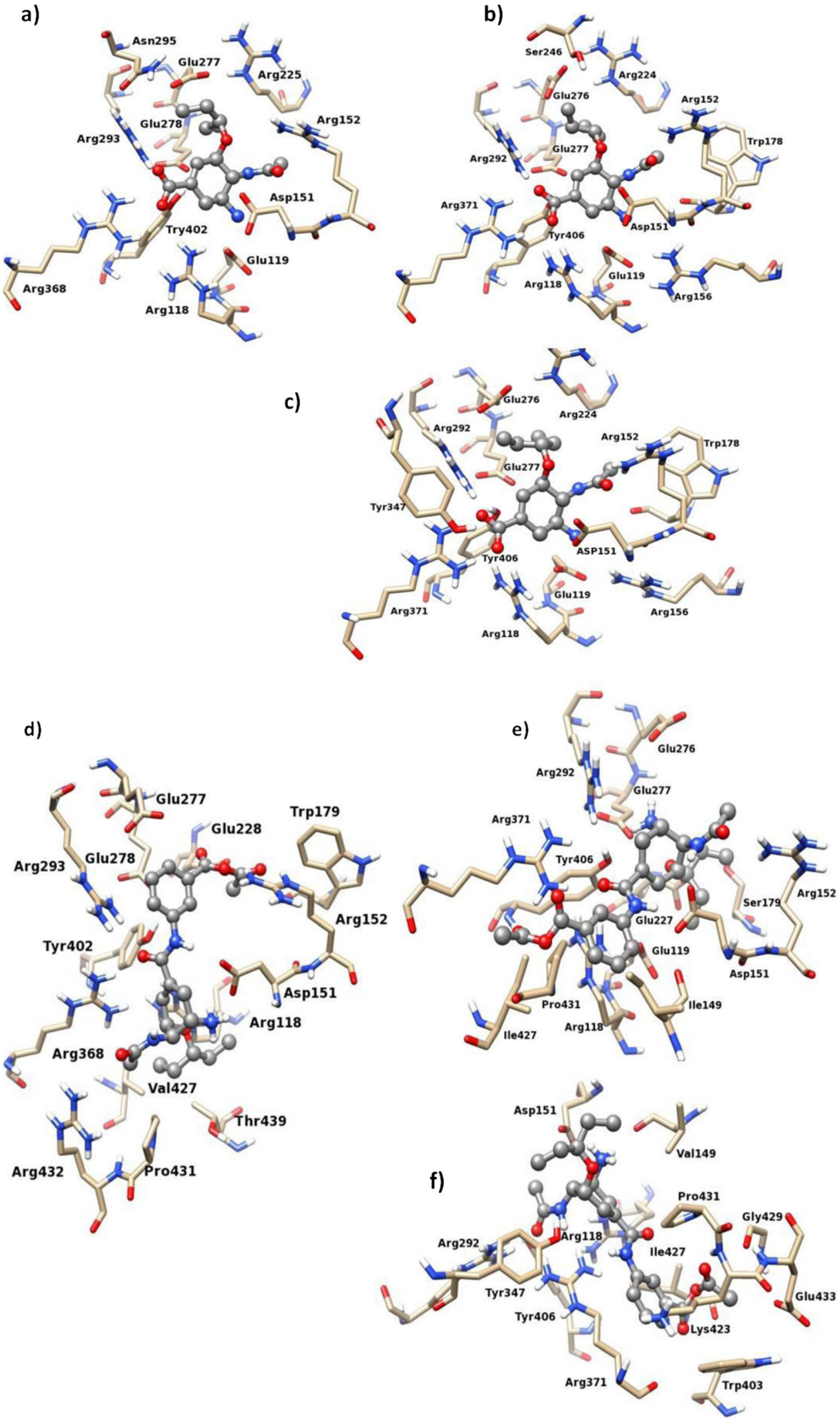
a)
Asn295
Glu277
Arg225
Arg152
Glu278
Arg293
Asp151
Try402
Glu119
Arg368
Arg118
b)
Ser246
Arg224
Glu276
Arg152
Trp178
Glu277
Arg292
Arg371
Asp151
Tyr406
Arg118
Glu119
Arg156
c)
Glu276
Arg224
Arg292
Arg152
Trp178
Glu277
Tyr347
ASP151
Tyr406
Glu119
Arg371
Arg156
Arg118
d)
Glu277
Trp179
Glu228
Arg293
Glu278
Arg152
Tyr402
Asp151
Arg118
Arg368
Val427
Thr439
Arg432
Pro431
e)
Glu276
Arg292
Glu277
Arg371
Tyr406
Ser179
Arg152
Glu227
Glu119
Asp151
Pro431
Ile149
Ile427
Arg118
f)
Asp151
Val149
Pro431
Gly429
Arg292
Arg118
Ile427
Tyr347
Glu433
Tyr406
Lys423
Arg371
Trp403

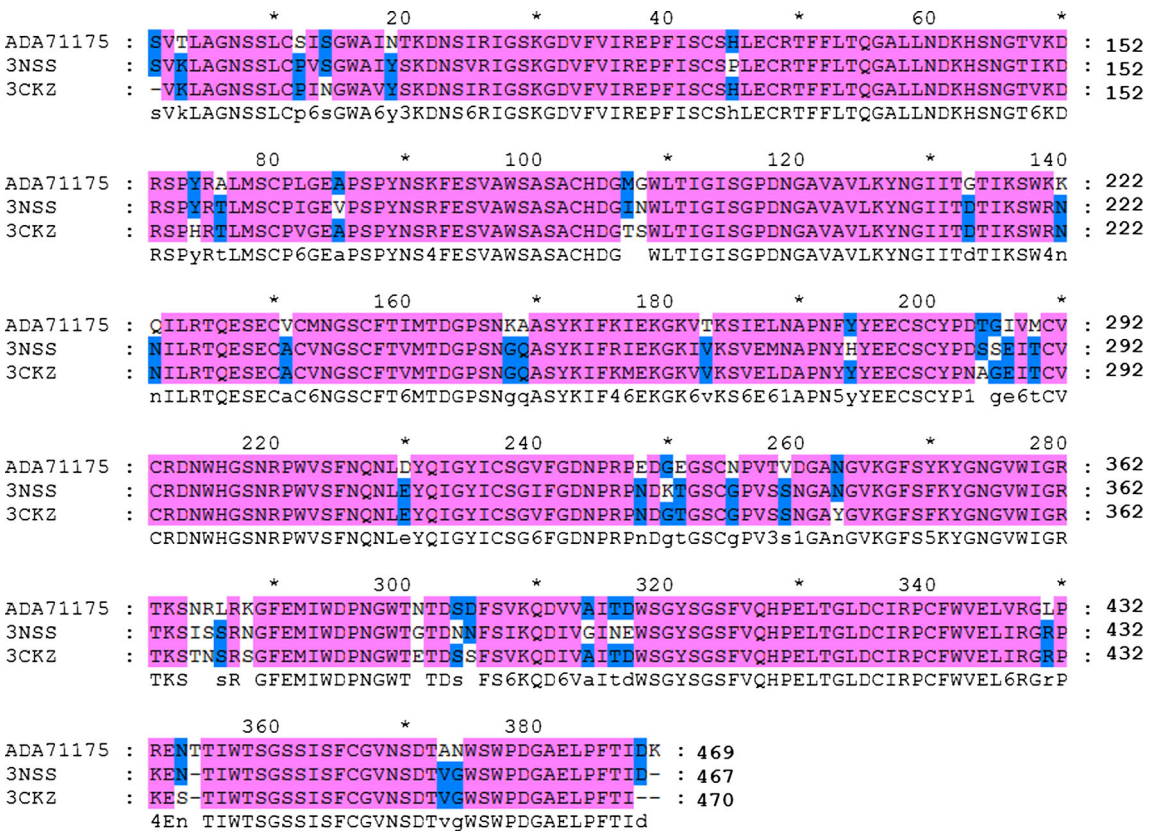

Fig. 2 Multiple alignment studies of three NA structures: two from PDB (wild type 3NSS and the crystal H27Y mutant 3CKZ) and one from GenBank (ADA71175 with H275Y and external binding-site mutations). The NA protein sequences were aligned using MUSCLE/Ebi. The figure was generated using GenDoc 2.0. Residues conserved between the sequences are highlighted with a *pink* background

depicted in Fig. 4c, the surfaces of the active sites of the NAs exhibit large structural differences. Thus, mutations outside the active site of NA change the shape of ADA71175. These changes have been observed for various NA subtypes, although the residues at the active site of NA are highly conserved among the different NAs [33]. Variations in the shape of the active site could be associated with ligand-recognition phenomena; however, little information is available on this topic because these issues have barely been explored for this protein. The number of oseltamivir-resistant cases has increased since the oseltamivir-resistant influenza viruses of the 2009 AH1N1 pandemic were first detected. Thus, in our study, we focused on the shape and size of the active site to explain the large number of cases that do not exhibit mutations of the active site of NA [15, 27] to explain those cases in which the NA H275Y mutation is not observed.

The structural variations in the shape of the active site of NA (Fig. 3b) can be explained in terms of residue mutations at H275 and the influence of neighboring mutated residues located outside the binding site due to either charge or hindrance effects associated with their side chains, which induce conformational changes, as has been reported for other proteins [34]. The mechanism by which mutations outside the binding site influence the binding site of NA has not been clarified; however, it is clear that structural changes can be induced and mediated by the types of residues that modify the active sites of the protein [35]. Figure 2 presents a large number of mutations present in ADA71175, including the H275Y mutation; these mutations change the shape of the active site (Fig. 3a), as we have recently reported [16]. One example of structural changes caused by residue mutations is the H275Y mutation of NA; this mutation induces conformational changes in the side chain of Glu276, which result in repulsive effects 2 Å into the binding site, caused by the carboxyl group's orientation with respect to the hydrophobic group of oseltamivir [8]. This scenario explains the resistance of NA to oseltamivir [8] and hence the recognition of oseltamivir; however, there may be another resistance mechanism that is not associated with H275Y mutation, as previously reported by our research group [15]. For this reason, we performed a docking study to explore the binding poses and the binding free energies of a set of mono- and disubstituted aryl derivatives of oseltamivir on the wild-type (3NSS) and mutated NA in the H275Y residue (ADA71175), as summarized in Table 1, which

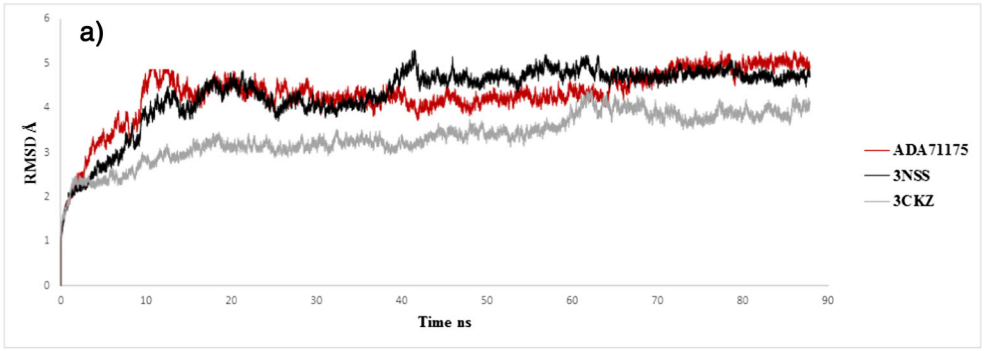

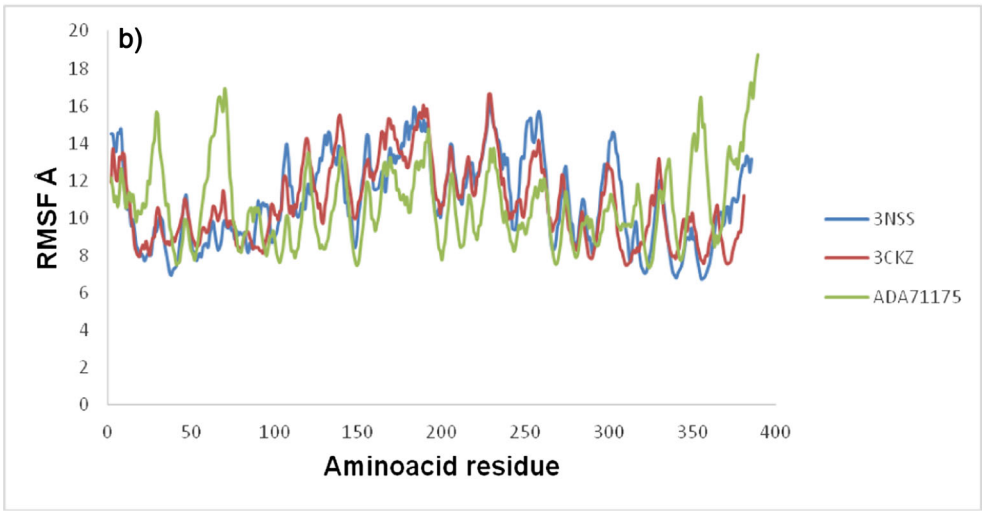

Fig. 3 **a** Root-mean-square deviations (RMSD) of the wild-type (3NSS) and mutant (PDB: 3CKZ and GenBank: ADA71175) NA structures that were submitted to MD simulation. The plots depict the convergences of the three investigated proteins. **b** Root-mean-square fluctuations (RMSF) of the target proteins

also includes many other mutations we have recently investigated [15]. This study was performed with the objective of exploring the possibility of targeting a cluster of conserved Arg residues (118, 292, and 371) [20] in order to design new compounds.

The predicted binding free energy values of oseltamivir show greater affinity for NA (3NSS), as has been reported elsewhere [15], than for NA mutants in both the native and refined structures. The recognition properties of oseltamivir on the NA structures indicate that the pentoxy group is positioned forward of Glu277 (Fig. 1), which reproduces the binding pose reported elsewhere [7]. As summarized in Table 1, the oseltamivir derivatives consistently reached the Arg cluster of the NA natives regardless of the position and type of substituent, and exhibited the lowest free energy values for ligand **45**, which possesses a group with a large volume and has the capacity to form three hydrogen bonds as an acceptor. In this sense, because one native conformation of the protein could exhibit structural behaviors that are dependent on the experimental conditions, which could cause the Arg cluster to be hidden from the oseltamivir-binding site, we employed an NA structure obtained from the MD simulations as a monomer and attempted to slightly deform the binding site without any structural perturbation; the resulting pattern of recognition appeared to be the same as that for the native NA structure because the Arg cluster was (again) reached consistently (Table 2). For example, the docking results for oseltamivir on either the native structure 3NSS or the structure subjected to MD simulations revealed electrostatic interactions between the carboxylate group of oseltamivir and the cluster of Arg residues (118, 292, and 371); see Figs. 1b and 5a. In addition, there are other two electrostatic interactions between Glu119 or Asp151 and the NH_3^+ group of oseltamivir. These electrostatic interactions are important for orienting the binding mode of oseltamivir. Moreover, there is a hydrogen-bond interaction between the carbonyl oxygen of the acetyl group of oseltamivir and Arg152, whereas the remaining residues interact with each other to stabilize the binding site, as reported by Karthick et al. [35]. However, when ADA71175 was subjected

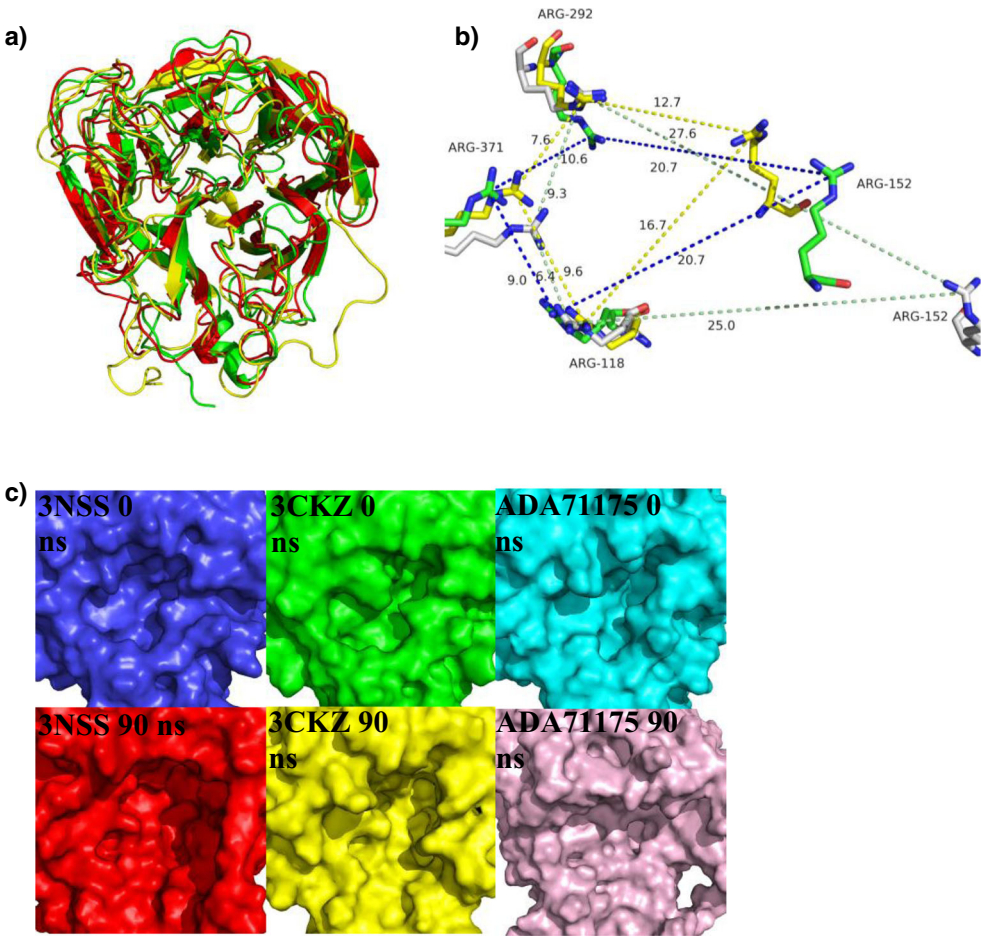

Fig. 4 **a** Alignment of 3NSS (*red*), 3CKZ (*green*), and ADA71175 (*yellow*). **b** Distances (Å) between certain important amino acids in the Arg cluster (Arg118, Arg371, Arg292, and Arg152). **c** 3D structural shapes of the pockets of wild-type NA (3NSS) and NA mutants (3CKZ/ADA71175) after refinement by MD simulation at 90 ns. These 3D structural properties of NA reflect the influence of neighboring mutated residues outside the binding site and by MD simulations using only the NA monomer

to MD simulations, the docking results demonstrated that the data are not reproducible in the presence of the NA H275Y mutation, as reported by Collins et al. [8]; this is because oseltamivir has a different mode of binding, and its functional groups COO^- and NH_3^+ lose their electrostatic interactions with the arginine assembly (118, 292, and 371) as well as with Asp152 and Glu119, respectively. As shown in Fig. 5b, the electrostatic interactions between the carboxylate group of oseltamivir and the Arg residues of ADA71175 do not occur; instead of these interactions, the NH_3^+ and NH groups of acetyl oseltamivir undergo hydrogen-bonding interactions with Glu276 and Tyr406. These interactions modify the oseltamivir-binding mode and cause the affinity for the NA to decrease. For this reason, we focused on the design of aryl-oseltamivir derivatives, which could strengthen the repulsion caused by H275Y and could be accommodated despite the presence of many mutations outside the binding site. The docking results indicated that aryl-oseltamivir derivatives have better affinity than oseltamivir for the NA of the influenza AH1N1 virus. Surprisingly, in general, the aryl-oseltamivir derivatives maintained the same binding modes as those in which oseltamivir is accommodated in wild-type NA [8]. Importantly, despite the fact that all aryl-oseltamivir derivatives have greater affinities than oseltamivir for both wild-type and mutated NA, the NH_3^+ group of each aryl-oseltamivir derivative does not interact with Glu119. This finding means that modifying the COO^- group of oseltamivir by adding a bulky group could affect the binding pose of NH_3^+, even though all aryl-oseltamivir derivatives showed the same binding mode to both proteins (3NSS and ADA71175), reaching the Arg cluster though the aryl moieties, which participate in cation–π interactions. On the NA structures subjected to MD simulations, these aryl-oseltamivir compounds yield ΔG results with high affinity values for compounds **7** (−9.36/−8.06 kcal mol^{-1}), **16** (−9.52/−9.52 kcal mol^{-1}), and **28** (−9.25/−8.22 kcal mol^{-1}); indeed, these compounds exhibited the greatest affinities (Table 2) for both investigated proteins.

Table 1 The binding free energy (ΔG) values of aryl-oseltamivir derivatives tested on wild-type NA and NA mutants in their native structures

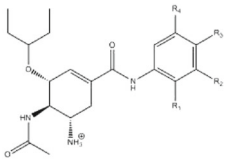

Ligand	Sustitution				Neuraminidase					
					3NSS		ADA71175		3CKZ	
	R1	R2	R3	R4	ΔG kcal mol^{-1}	π-cation	ΔG kcal mol^{-1}	π-cation	ΔG kcal mol^{-1}	π-cation
OST	---	---	---	---	-8.47	R224, R371, R118, R152, R292	-6.33	R225,R152, R293, R368, R118	-9.52	R292, R371, R224, R118, R152
1	NH_2	H	H	H	-8.31	R224, R152, R371, R118, R152	-7.7	R152, R293, R118, R368	-9.29	RG292, R118, R371, R430
2	H	NH_2	H	H	-7.96	R292,R371, R118	-8.71	R368, R118, R432	-10.24	R118, ARG371, R430
3	H	H	NH_2	H	-8.61	R292, RG371, RG118,	-8.26	R368, R432	-9.38	R371, R430
4	OH	H	H	H	-8.18	R224, R292, R152, R118, R371	-8.7	R225, R293, R152, R368, R118	-9.25	R292, R371, R118, R430
5	H	OH	H	H	-7.89	R224, R292, R371, R118	-7.48	R368, R118, R432	-9.99	R371, R118, R428, R430
6	H	H	OH	H	-7.2	R292, R371, R118, R224, R152	-7.81	R368, R118, R432	-9.41	R371, R118, R371, R430, R428
7	OCH_3	H	H	H	-7.6	R292, R118, R371, R224, R152	-8.03	R432, R118, R368	-8.47	R292, R371, R118, R430
8	H	OCH_3	H	H	-7.79	R292, R371, R118, R224	-7.78	R225, R152, R293, R118,R368	-9.66	R371, R118, R430
9	H	H	OCH_3	H	-8.06	R224, R152	-7.65	R225, R152, R293, R368, R118	-7.7	R371, R118, R152, R224
10	F	H	H	H	-8.6	R371, R118, R292, R430	-7.85	R368, R118, R432	-8.77	R430, R118, R292, R371
11	H	F	H	H	-7.8	R118, R371	-7.63	R368, R118, R432	-9.77	R371, R118, R430
12	H	H	F	H	-8.3	R152, R118, R371, R430	-7.53	R225, R293, R152	-7.84	R118, R430, R371, R292
13	Cl	H	H	H	-8.51	R152, R118, R371	-7.7	R118, R368, R293	-8.54	R430, R118, R371, R292
14	H	Cl	H	H	-8.88	R152, R371, R118	-8.18	R118, R432, R368	-8.92	R152, R118, R371,R292, R224
15	H	H	Cl	H	-8.2	R224	-8.12	R293,R152, R225	-7.85	R118, R430, R292
16	I	H	H	H	-8.66	R371, R118 , R224,R152	-7.73	R118, RG368, R293	-8.92	R118, R371, R292
17	H	I	H	H	-9.1	R371, R118, R152	-8.57	R118, R368, R293, R225	-9.35	R428, R118, R371,R292
18	H	H	I	H	-8.36	R371, R118, R292, R156,	-8.44	R293, R247, R152, R225	-7.88	R224, R118, R152, R156

The docking results suggest that the high affinity of all aryl-oseltamivir derivatives for NA subjected to MD simulations can be attributed to the interaction of ligands (aryl moieties) with residues (Arg118, Arg292, and Arg371) that carry a positive charge. This conclusion can be drawn because all aryl-oseltamivir derivatives are characterized by the possession of an aromatic moiety at the carboxylate group that is capable of forming π-π interactions or π-cation interactions with the aromatic or positively charged residues, respectively, that are present in the NA pocket site (see Fig. 6). It has been demonstrated that the incorporation of an aryl group into the structure of some enzyme inhibitors improves their affinity; this occurs, for example, for some acetylcholinesterase inhibitors [36] or anti-inflammatory agents [37, 38] acting as

Table 1 (continued)

						R152				
19	Br	H	H	H	-8.54	R371, R118, R224, R152	-7.99	R118, R368, R368, R293	-8.56	R292,R118, , R371
20	H	Br	H	H	-8.96	R118, R371, R224, R152	-8	R152, R118, R368, R393	-9.12	R118, R152, R224, R292, R371
21	H	H	Br	H	-8.31	R224	-8.39	R152, R225, R293	-8.18	R292, R224, R371, R118
22	NO_2	H	H	H	-8.99	R152, R224, R292, , R371	-8.06	R152, R225, R293	-9.05	R224, R292, R371, R119, R152
23	H	NO_2	H	H	-8.81	R152, R156, R292, R371	-8.22	R225, R152, R293, R368, R118	-8.78	R292, R371, R118, R430, R428
24	H	H	NO_2	H	-8.84	R224	-7.66	R225, R152, R293	-8.26	R224
25	CN	H	H	H	-8.74	R152, , R430, R156, R118, R371, R292	-8.35	R293, R225, R152	-8.39	R292, R371, R430, R118
26	H	CN	H	H	-9	R152, R156, R371, R118	-8.02	R293, R152, R368, R118	-9.1	R292, R371, R118, R430
27	H	H	CN	H	-9.19	R224, R229	-8.33	R225,R152, R293	-8.65	R224
28	COOH	H	H	H	-9.03	R152, R224, R292, R371, R118	-7.74	R293, R432, R368, R118	-9.59	R292, R371, R224, R118, R152
29	H	COOH	H	H	-9.22	R152, R156, R118, R371	-8.13	R152, R225	-9.37	R118, R371, R292
30	H	H	COOH	H	-8.37	R224, R152	-7.57	R152, R225, R293	-7.88	R292, R224, R371, R152, R118, R156
31	CH_3	H	H	H	-8.7	R152, R371, R118	-7.74	R293, R368, R118	-8.71	R224, R152, R292, R118, R371
32	H	CH_3	H	H	-8.75	R152, R371, R118, R156	-7.82	R293,R368, R118	-8.72	R118, R292, R371, R430, R428
33	H	H	CH_3	H	-8.14	R224, R292	-7.92	R152,R225 ,R293	-8.38	R118,R292, R371, R430,
34	H	H	H	H	-8.62	R152, R371, R118, R156,	-7.5	R225, R152, R293	-8.48	R156, R224, R152, R156, R118, R292, R371
35	SOOOH	H	H	H	-8.63	R292, R224, R152	-8.77	R152, R225, R293	-9.51	R292, R118, R371, R430
36	H	SOOOH	H	H	-9.17	R292, R371, R118, R152, R430	-8.33	R368, R118, R293, R225, R152	-9.2	R224, R292, R118, R371
37	H	H	SOOOH	H	-8.58	R224	-7.74	R293, R225, R152	-7.98	R156, R224
38	OH	H	NO_2	H	-8.27	R224	-8.08	R225, R152, R293, R368, R118	-7.79	R118, R152, R371, R292, R224
39	OH	H	CH_3	H	-8.38	R292, R152, R371, R156	-8.33	R152, R225, R293, R368, R118	-8.34	R118, R371, R152, R292, R224, R371
40	OH	H	NO_2	Cl	-7.83	R224, R152	-8.55	R152, R225, R293,R368, R118	-8.26	R118, R152, R371, R292, R224
41	H	H	OH	COOH	-8.34	R371,R118, R152, R430	-7.63	R152, R225, R156	-9.07	R371, R292, R118
42	H	OH	COOH	H	-8.17	R224	-7.52	R152, R225, R293	-7.28	R118, R152, R371, R224, R292
43	OH	H	H	CH_3	-9.25	R371 , R118,R152	-8.34	R152, R225, R293, R368, R118	-9.06	R156, R118, R152, R371, R224
44	$COOCOCH_3$	H	H	H	-8.69	R292, R152,	-8.17	R225, R152,	-8.63	R118, R371,

cyclooxygenase inhibitors. This behavior arises because π–π and π-cation interactions are very important for protein recognition and ligand–protein-complex stabilization, as is evident in Fig. 6a, which illustrates how the binding mode

Table 1 (continued)

						R156, R118, R371		R225, R293		R292
45	H	$COOCOCH_3$	H	H	-9.47	R224, R152, R371, R118	-9.23	R225, R152, R293, R368, R118	-10.49	R118, R371, R371, R292
46	H	H	$COOCOCH_3$	H	-9.38	R224, R152,	-8.52	R152, R225, R293	-8.22	R224
47	$N(CH_3)_2$	H	H	H	-8.13	R292, R152, R371, R156, R118	-7.77	R293, R118, R368,	-8.46	R430, R118, R371, R292
48	H	$N(CH_3)_2$	**H**	**H**	-8.68	R152, R371,R118	-7.96	R293, R368, R118	-8.89	R118, R371, R292, R224
49	H	H	$N(CH_3)_2$	H	-8.12	R224, R292, R152, R371, R118, R430	-7.87	R152, R225, R293	-7.4	R118, R292, R371, R430
50	CH_3	H	H	H	-8.71	R152, R156, R118, R371	-7.64	R118, R368, R293	-8.63	R118, R224, R292, R152, R371
51	H	CH_3	H	H	-8.77	R152, R371, R118	-7.84	R368, R118, R432, R428	-8.76	R152, R156, R224, R118, R371
52	H	H	CH_3	H	-8.17	R224, R152	-7.8	R152, R225, R293	-8.19	R371, R292, R118, R430
53	CH_2CH_3	H	H	H	-8.7	R152, R371, R118, R156	-7.84	R118, R293, R368	-8.97	R292, R224, R118, R156
54	H	CH_2CH_3	H	H	-8.86	R152, R371, R118	-8.12	R432, R118, R368, R428	-9.32	R430, R118, R292, R371
55	H	H	CH_2CH_3	H	-8.26	R224	-8	R152, R225, R293	-8.52	R118, R292,R371, R430, R430
56	$CH_2CH_2CH_3$	H	H	H	-9.21	R371, R118, R152	-7.86	R293, R368, R118	-9.37	R371, R292, R118, R152, R156
57	H	$CH_2CH_2CH_3$	H	H	-9.05	R371, R118, R152	-8.25	R225, R152, R293, R156, R368, R118	-9.4	R371, R292, R118
58	H	H	$CH_2CH_2CH_3$	H	-8.23	R224, R152	-7.91	R225, R152, R293	-8.47	R118, R292, R371, R428, R430
59	CH(CH3)2	H	H	H	-8.25	R292,R118, R371, R156, R152	-8.19	R293, R368, R118	-8.6	R292, R371, R118
60	H	$CH(CH_3)_2$	H	H	-9.1	R371, R118, R156, R152, R292	-8.39	R152, R293, R368, R118	-9.57	R118, R292, R371, R428, R430
61	H	H	$CH(CH_3)_2$	H	-8.48	R224, R152	-7.81	R432, R368, R368, R118	-7.8	R118, R371, R292
62	H	OCH_3	NO_2	H	-8.38	R224	-7.81	R43,R368, R118	-8.15	R118, R371, R292
63	H	OH	NO_2	H	-8.61	R292, R224,R371, R118, R430, R152	-7.69	R225, R152	-7.79	R224
64	H	$N(CH_3)_2$	NO_2	H	-8.45	R224, R152	-7.36	R293, R152, R225	-8.08	R118, R371, R325, ASN325 R292
65	H	Cl	NO_2	H	-8.82	R224	-7.56	R225, R152, R293	-8.4	R224
66	H	I	NO_2	H	-9.01	R224	-7.87	R293, R225, R152	-8.71	R152
67	H	Br	NO_2	H	-8.96	R224, R152	-7.7	R225, R152	-8.6	R152, R224
68	H	OCH_3	COOH	H	-8.13	R224	-6.98	R293, R225, R152	-8.04	R118, R152, R371
69	H	OH	COOH	H	-8.17	R224	-7.49	R293,R225, R152	-7.2	R152, R224
70	H	$N(CH_3)_2$	COOH	H	-8.21	R224	-7.29	R225, R223, R225, R152	-8.2	R118, R371, R292

of ligand **16** on wild-type NA is established through various types of interactions: π-cation interactions with Arg118 and Arg371; electrostatic interactions with Arg371; and hydrogen bonds with Arg118, Agr152, Glu119 and Tyr406. In addition,

Table 1 (continued)

71	H	Cl	COOH	H	-8.41	R224	-7.35	R293, R225, R152	-8.14	R152, R118, R224, R292, R371
72	H	I	COOH	H	-8.6	R224	-7.65	R225, R152	-8.41	R152, R118, R224, R292, R371
73	H	Br	COOH	H	-8.57	R224, R152	-7.64	R293, R225, R152	-8.36	R118, R152, R224, R292, R371
74	H	NH_2	COOH	H	-8.17	R152, R118, R371,R292, R224	-7.4	R225, R152	-7.46	R118, R430, R371, R292
75	H	CH_3	COOH	H	-8.56	R224	-7.65	R225, R152, R293	-7.88	R152, R224
76	H	CH_2CH_3	COOH	H	-8.49	R224	-7.62	R225, R152, R293	-8.44	R118, R371
77	H	$CH_2CH_2CH_3$	COOH	H	-8.22	R224, R152	-7.51	R152, R225	-8.46	R118, R292, R371
78	H	$CH(CH_3)_2$	COOH	H	-8.37	R224	-7.73	R225, R152, R293	-8.41	R118, R292,R371
79	H	$CH_2CH(CH_3)_2$	COOH	H	-8.28	R224, R152	-7.62	R225, R152, R293	-8.58	R118, R152, R224, R292, R430, R374
80	H	$C(CH_3)_3$	COOH	H	-8.52	R224	-7.89	R225, R152, R293	-7.98	R152, R118, R224, R292, R371
81	H	OCH_3	OCH_3	H	-8.17	R430, R152, R118, R371, R292,R224	-7.3	R225, R152, R293	-7.79	R430, R371, R118, R292
82	H	OH	CH2OH	H	-8.51	R292, R371, R118, R152, R224, R430	-7.45	R225, R152, R293	-8.21	R292, R371, R118, R430
83	H	CH_2OH	$N(CH_3)_2$	H	-7.83	R292,R371, R118, R152, R224	-8.02	R225, R152, R293	-7.32	R224, R292, R152
84	H	Cl	CH_2OH	H	-8.42	R224,R152	-7.81	R225, R152,R293	-8.95	R118, R371, R292
85	H	I	CH_2OH	H	-8.51	R224, R292	-7.98	R225, R152, R293	-8.52	R292, R224, R371, R118

16 reaches ADA71175 (Figs. 5b and 6) by means of several interactions similar to those observed for wild-type NA, such as π-cation interactions with Arg118; hydrogen bonds with Arg152, Asp151, Glu119 and Tyr406; and several hydrogen bonds with the backbones of the residues that control the conformation of the active site. It is important to note that aryl-oseltamivir derivatives interact not only with the residues at the NA active site but also with residues with the I149V mutation. These findings suggest that these aryl-oseltamivir derivatives could be recognized for the entire group of NAs 1 and 2, which Wang et al. [39] have related to the 150-loop, which is preserved for all subtypes of the NA group except that of the 2009 pandemic; the latter has a I149V mutation, endowing it with properties characteristic of group 2. Rudrawar S. et al. [40] have demonstrated that the substitution of one aliphatic chain by an aromatic ring of NA inhibitors provides greater inhibition, as estimated in their in silico studies. In our docking studies, we found different affinity values for the aryl-oseltamivir derivatives in the NA active site on native NA than for the NA snapshots retrieve from the MD simulations, indicating that including an aryl moiety in oseltamivir causes some electrostatic interactions with the Arg cluster to be lost; however, other difficult-to-establish interactions are formed, such as π-cation interactions (Table 3).

The docking results suggest that the high affinities of all aryl-oseltamivir derivatives for NA subjected to MD simulations can be attributed to the interaction of ligands (aryl moieties) with residues (Arg118, Arg292, and Arg371) that carry a positive charge. This conclusion can be drawn because all of the aryl-oseltamivir derivatives are characterized by the presence of an aromatic moiety at the carboxylate group that is capable of forming π–π interactions or π–cation interactions with the aromatic or positively charged residues, respectively, that are present in the pocket site of NA (see Fig. 6). It has been demonstrated that the incorporation of an aryl group into the structures of some enzyme inhibitors improves their affinities; this occurs, for example, for some acetylcholinesterase inhibitors [36] or anti-inflammatory agents [37, 38] acting as cyclooxygenase inhibitors. This behavior arises because π–π and π–cation interactions are very important for protein recognition and ligand–protein complex stabilization, as is

Table 2 Binding free energy (ΔG) values of aryl-oseltamivir derivatives tested on wild-type NA and NA mutants subjected to MD simulations (snapshots at 50 ns)

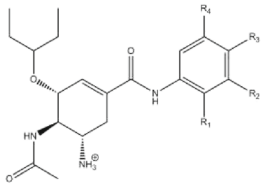

Ligand	Sustitution				Neuraminidase					
					3NSS		ADA71175		3CKZ	
	R1	R2	R3	R4	ΔG kcal mol^{-1}	π-cation	ΔG kcal mol^{-1}	π-cation	ΔG kcal mol^{-1}	π-cation
OST	---	---	---	---	-8.41	---	-5.04	---	---	---
1	NH_2	H	H	H	-8.35	R118,371	-7	R118	-7.84	R118,152
2	H	NH_2	H	H	-9.28	R118,371	-7.83	R224	-7.9	R152
3	H	H	NH_2	H	-8.64	R224	-7.71	R224	-8.71	R118,152
4	OH	H	H	H	-7.75	----	-7.86	---	-8.31	R224
5	H	OH	H	H	-9.32	R118,371	-7.78	R224	-8.1	R152
6	H	H	OH	H	-8.77	R224	-7.86	R118	-8.16	R152
7	OCH_3	H	H	H	-9.36	R118,371	-8.06	R224	-7.83	R152
8	H	OCH_3	H	H	-9.19	R118,371	-7.99	R118,371	-7.8	R118,152,371
9	H	H	OCH_3	H	-8.12	R224	-8.15	R118,371	-7.83	R224
10	F	H	H	H	-8.14	R292,371	-7.41	R118	-7.77	R118,224
11	H	F	H	H	-8.23	R292,371	-8.23	R224	-8.11	R118,152
12	H	H	F	H	-6.92	---	-7.52	R224	-7.81	R152
13	Cl	H	H	H	-9.48	R118,371	-8.47	R118	-7.3	R224,152
14	H	Cl	H	H	-9.74	R118,371	-8.25	R224	-6.8	R224,152
15	H	H	Cl	H	-8.44	R224	-8.63	R224	-7.92	R224,152
16	I	H	H	H	-9.52	R118,371	**-9.52**	R118	-8.01	R152
17	H	I	H	H	-9.8	R118,371	-8.51	R224	-7.37	R118,224,152
18	H	H	I	H	-8.42	R224	-9.05	R224	-8.25	R224,152
19	Br	H	H	H	-9.46	R118,371	-8.13	R118	-7.76	R118,224,152
20	H	Br	H	H	-9.83	R118,371	-8.23	R224	-6.98	R371
21	H	H	Br	H	-8.84	R292	-8.74	R224,292	-8.38	R224,152
22	NO_2	H	H	H	-11.21	R118,292,371	-7.72	R118	-7.14	R152
23	H	NO_2	H	H	-9.29	R118,371	-8.39	R118	-8.32	R224,152
24	H	H	NO_2	H	-9.17	R224	-7.83	R224	-7.91	R118,224,152,371
25	CN	H	H	H	-9.69	R118,371	-8.3	R118	-7.49	R118,152,371
26	H	CN	H	H	-9.51	R118,371	-7.55	R118	-7.16	R224,152, 371
27	H	H	CN	H	-9.67	R224,292	-7.49	R118,371	-7.47	R152
28	COOH	H	H	H	-9.25	R118,292,371	-8.22	R118	-8.03	R118,152
29	H	COOH	H	H	-8.98	R118,371	-8.28	R118,371	-9.02	R118,152,371
30	H	H	COOH	H	-8.9	R224	-7.5	R224	-6.97	R152,371
31	CH_3	H	H	H	-9.35	R118,371	-7.37	R118	-8.28	R118,224,152

evident in Fig. 6, which illustrates how the binding mode of ligand **16** on wild-type NA is established through various types of interactions: π–cation interactions with Arg118 and Arg371; electrostatic interactions with Arg371; and hydrogen bonds with Arg118, Agr152, Glu119, and Tyr406. In addition, **16** reaches ADA71175 (Fig. 6b) by means of several interactions similar to those observed for wild-type NA, such as π–cation interactions with Arg118; hydrogen bonds with Arg152, Asp151, Glu119, and Tyr406; and several hydrogen bonds with the backbones of the residues that control the

Table 2 (continued)

32	H	CH_3	H	H	-7.63	R118	-7.2	R118,371	-8.14	R118,152
33	H	H	CH_3	H	-7.69	R118,371	-7.35	R224	-7.75	R118,152
34	H	H	H	H	-7.99	R118,371	-7.53	R118	-7.23	R224,152
35	SOOOH	H	H	H	-10.13	R118,292,371	-8.37	R118,371	-8.4	R118,152
36	H	SOOOH	H	H	-8.9	R118,371	-9.01	R118,371	-7.05	---
37	H	H	SOOOH	H	-8.17	R118,371	-8.8	R224	-8.01	R152
38	OH	H	NO_2	H	-7.75	R118,371	-7.8	R371	-6.77	R224
39	OH	H	CH_3	H	-7.55	R118,371	-7.01	R224,292	-8.64	R224,152
40	OH	H	NO_2	Cl	-7.63	R118	-7.16	R118,371	-7.11	---
41	H	H	OH	COOH	-7.66	R118,371	-7.88	R118,371	-6.99	R152,371
42	H	OH	COOH	H	-7.54	R118	-7.86	R118,371	-6.77	R224
43	OH	H	H	CH_3	-6.3	R118	-7.01	R224	-6.94	---
44	$COOCOCH_3$	H	H	H	-8.75	R118,371	-7.56	---	-7.65	R152
45	H	$COOCOCH_3$	H	H	-9.78	R118,371	-8.69	R292	-7.47	---
46	H	H	$COOCOCH_3$	H	-7.64	R371	-7.24	R118	-7.36	R224
47	$N(CH_3)_2$	H	H	H	-7.3	---	-6.06	---	-8.25	R118,152
48	H	$N(CH_3)_2$	H	H	-7.73	R371	-6.86	R118,Y406	-6.68	R224
49	H	H	$N(CH_3)_2$	H	-7.31	---	-7.93	---	-6.84	R224
50	CH_3	H	H	H	-7.48	---	-7.59	---	-8.08	R224,152
51	H	CH_3	H	H	-7.01	---	-6.77	---	-7.7	R152
52	H	H	CH_3	H	-7.33	---	-7.34	R118	-7.63	R118,224,152
53	CH_2CH_3	H	H	H	-8.49	---	-7.38	R118	-7.16	R118,224,152
54	H	CH_2CH_3	H	H	-7.95	R118,371	-7.56	---	-7.22	---
55	H	H	CH_2CH_3	H	-7.61	---	-6.94	R118	-8.75	R152
56	$CH_2CH_2CH_3$	H	H	H	-8.11	R118,371	-6.68	---	-8.18	R118,152,371
57	H	$CH_2CH_2CH_3$	H	H	-8.3	R118	-7.22	---	-6.74	---
58	H	H	$CH_2CH_2CH_3$	H	-7.59	R118	-7.7	R118	-8.69	R152
59	CH(CH3)2	H	H	H	-8.48	R224	-7.12	R224	-8.42	R224,152
60	H	$CH(CH_3)_2$	H	H	-7.95	---	-6.54	---	-8.32	R224,152
61	H	H	$CH(CH_3)_2$	H	-8.22	R118	-6.32	R118	-7.55	R224,152
62	H	OCH_3	NO_2	H	-8.32	R118	-8.34	R118,371	-7.46	R118,152,371
63	H	OH	NO_2	H	-9.19	R118,371	-7.22	---	-7.72	R224,152
64	H	$N(CH_3)_2$	NO_2	H	-9.06	R118,371	-7.73	R224	-7.81	R152,371
65	H	Cl	NO_2	H	-9.45	R118,371	-8.0	R371	-7.52	R152,371
66	H	I	NO_2	H	-9.05	R118,Y406	-7.66	R224	-7.3	R152
67	H	Br	NO_2	H	-8.87	R118,292	-7.51	R118	-7.71	R152,371
68	H	OCH_3	COOH	H	-8.39	R118,371	-7.49	---	-7.63	R152,371
69	H	OH	COOH	H	-6.78	--	-6.7	R118	-7.62	R118,224,152,371
70	H	$N(CH_3)_2$	COOH	H	-9.23	R118,371	-7.57	---	-7.65	R118,224,152,371
71	H	Cl	COOH	H	-8.74	R118,371	-6.89	---	-6.63	R224,371
72	H	I	COOH	H	-9.14	R371	-8.53	R118,371	-8.35	R118,224,152,371
73	H	Br	COOH	H	-9.05	R118,371	-8.29	R118,371	-6.99	R224,371
74	H	NH_2	COOH	H	-8.88	R152	-8.46	R118,371	-7.33	R118,224,152,371
75	H	CH_3	COOH	H	-7.86	R118,371	-6.92	---	-7.65	R118,224,152
76	H	CH_2CH_3	COOH	H	-9.08	R118,371	-8.36	R118,371	-6.67	R371
77	H	$CH_2CH_2CH_3$	COOH	H	-8.79	R118	-7.45	R371	6.94	R118,224,371
78	H	$CH(CH_3)_2$	COOH	H	-9.71	R118,371	-7.25	---	-7.8	R118,224,152,371
79	H	$CH_2CH(CH_3)_2$	COOH	H	-8.26	R118,371	-7.14	R371	-6.87	R224
80	H	$C(CH_3)_3$	COOH	H	-8.02	R118,371	-7.95	R118	-6.69	R371
81	H	OCH_3	OCH_3	H	-8.49	R118,371	-8.5	R118,371	-7.59	R224,152
82	H	OH	CH2OH	H	-7.78	---	-7.19	R118	-7.04	R224,152
83	H	CH_2OH	$N(CH_3)_2$	H	-9.04	R118	-7.81	R118	-6.42	---
84	H	Cl	CH_2OH	H	-9.04	R292,Y406	-7.99	R224	-6.54	R224,152
85	H	I	CH_2OH	H	-9.69	R118,292	-8.07	R224	-8.53	R224,152,371

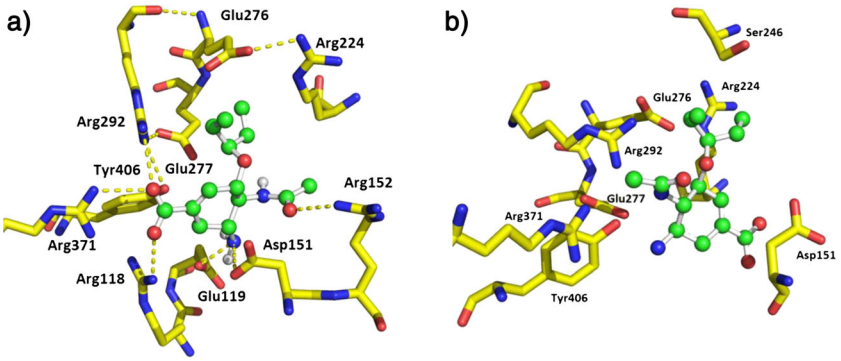

Fig. 5 **a** Oseltamivir binding mode on 3NSS; the carboxylate group of oseltamivir is oriented toward Glu277, whereas the carboxylate group is oriented toward the Arg cluster, in agreement with the literature [8]. **b** Oseltamivir binding mode on ADA71175, depicting how the binding pose is affected by NA mutations and MD simulations on NA monomers

conformation of the active site. It is important to note that aryl-oseltamivir derivatives interact not only with the residues at the active site of NA but also with residues with the I149V mutation. These findings suggest that these aryl-oseltamivir derivatives could be recognized by all group 1 and 2 NAs, which Wang et al. [39] have related to the 150-loop, which is preserved for all subtypes of the NA group except that associated with the 2009 pandemic; the latter has a I149V mutation, endowing it with properties characteristic of group 2. Rudrawar S. et al. [40] have demonstrated that the substitution

Table 3 Interactions of aryl-oseltamivir derivatives on NA via hydrogen bonds, π-cation interactions and electrostatic interactions between NA residues located within the active site (Arg118, 158, 292 and 371; Glu276 and 277; and Asp151) with ligands 7 and 16

Ligand	Hydrogen bonds						π-cation			Electrostatic
7	D151/*1	D151/*2	R152/*3	Y406/*4	R371/*4	R118/*6	R118/*5	R371/*5	R292/*5	NH_3^+/Glu277
16	D151/*1	D151/*2	R152/*3	Y406/*4	R371/*4	–	R118/*5	R371/*5	–	NH_3^+/Glu277

* 1 = NH amide

* 2 = NH acetyl

* 3 = acetyl oxygen

* 4 = amide oxygen

*5 = aromatic ring

*6 = O-methyl

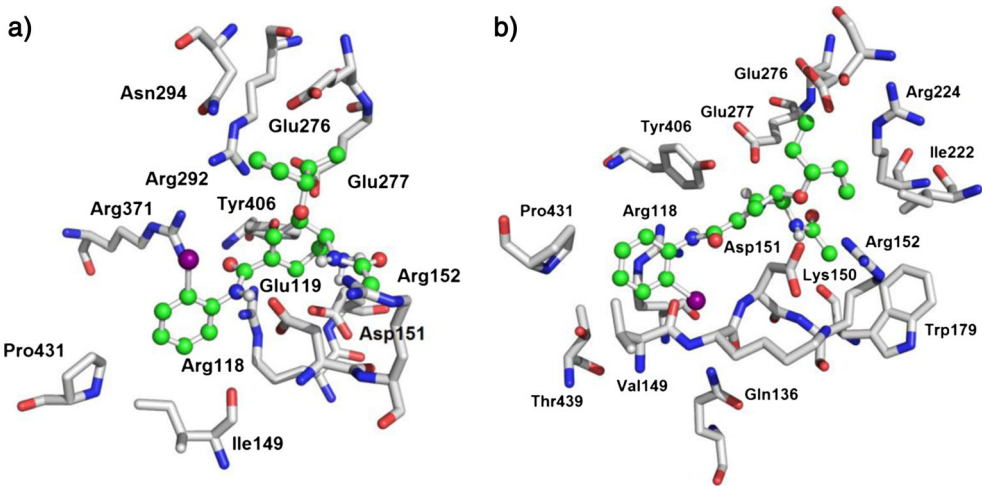

Fig. 6 **a** Binding mode of **16** on 3NSS, depicting the π-cation interaction between the aryl moieties of the ligands and the Arg cluster. **b** Binding mode of aryl-oseltamivir derivatives on ADA71175, depicting the π-cation interaction between the aryl moieties of the ligands and the Arg cluster. In both cases, the binding pose is identical for either wild-type NA or mutated NA

of one aliphatic chain by an aromatic ring of NA inhibitors provides greater inhibition, as estimated in their in silico studies. In our docking studies, we found different affinity values for the aryl-oseltamivir derivatives in the active site of native NA than the NA snapshots retrieved from the MD simulations, indicating that including an aryl moiety in oseltamivir causes the loss of some electrostatic interactions with the Arg cluster; however, other difficult-to-establish interactions are formed, such as π–cation interactions (Table 3).

In conclusion, in this study, we obtained evidence that adding an aromatic group may help to establish π–cation interactions that increase and maintain the affinity of the binding mode despite the presence of mutated NA. Hence, this series of oseltamivir derivatives could generate precursors that could be further optimized and developed to serve as novel lead compounds for the design and discovery of anti-influenza drugs. Furthermore, these aryl-oseltamivir derivatives are promising compounds for inhibiting the NA of the influenza A (H1N1) virus.

Acknowledgments The work was supported by grants from ICyTDF (Instituto de Ciencia y Tecnología del Distrito Federal), CONACYT (Consejo Nacional de Ciencia y Tecnología), CYTED (Programa Iberoamericano de Ciencia y Tecnología para el Desarrollo) and BEIFI (BECA DE ESTÍMULO INSTITUCIONAL DE FORMACIÓN DE INVESTIGADORES), SIP (secretaria de investigación y posgrado), COFAA (COMISIÓN DE OPERACIÓN Y FOMENTO DE ACTIVIDADES ACADEMICAS) from IPN (Instituto Politécnico Nacional, México).

References

1. Zhong S, MacKerell AD Jr (2007) J Chem Inf Model 47:2303–2315
2. Navarro-Polanco RA, Moreno Galindo EG, Ferrer-Villada T, Arias M, Rugby JR, Sanchez-Chapula JA, Tristani-Firouzi M (2011) J Physiol 589(Pt 7):1741–1753. doi:10.1113/jphysiol.2010.204107
3. Vijayan R, Sahai MA, Czajkowski T, Biggin PC (2010) Phys Chem Chem Phys 12:14057–14066
4. Demina A, Varughese KI, Barbot J, Forman L, Beutler E (1998) Blood 92:647–652
5. Nguyen AP, Downard KM (2013) Analyst 138:1787–1793
6. Chen LF, Dailey NJ, Rao AK, Fleischauer AT, Greenwald I, Deyde VM, Moore ZS, Anderson DJ, Duffy J, Gubareva LV, Sexton DJ, Fry AM, Srinivasan A, Wolfe CR (2011) J Infect Dis 203:838–846
7. Longtin J, Patel S, Eshaghi A, Lombos E, Higgins R, Alexander D, Olsha R, Doyle J, Tran D, Sarabia A, Lee C, Bastien N, Li Y, Low D, Boivin G, Gubbay J (2011) J Clin Virol 50:257–261
8. Collins PJ, Haire LF, Lin YP, Liu J, Russell RJ, Walker PA, Skehel JJ, Martin SR, Hay AJ, Gamblin SJ (2008) Nature 453:128–1261
9. Woods CJ, Malaisree M, Pattarapongdilok N, Sompornpisut P, Hannongbua S, Mulholland A (2012) J Biochem 51:4364–4375
10. Basha SH, Prasad RN (2012) BMC Res Notes 5:105
11. Sheu TG, Fry AM, Garten RJ, Deyde VM, Shwe T, Bullion L, Peebles PJ, Li Y, Klimov AI, Gubareva LV (2011) J Infect Dis 203:13–71
12. Esposito S, Molteni CG, Daleno C, Valzano A, Fossali E, Da Dalt L, Cecinati V, Bruzzese E, Giacchino R, Giaquinto C, Galeone C, Lackenby A, Principi N (2010) Virol J 7:202
13. Govorkova EA, Ilyushina NA, Marathe BM, McClaren JL, Webster RG (2010) J Virol 84:8042–8050
14. Zepeda HM, Perea-Araujo L, Zarate-Segura PB, Vázquez-Pérez JA, Miliar-García A, Garibay-Orijel C, Domínguez-López A, Badillo-Corona JA, López-Orduña E, García-González OP, Villaseñor-Ruíz I, Ahued-Ortega A, Aguilar-Faisal L, Bravo J, Lara-Padilla E, García-Cavazos RJ (2010) J Clin Virol 48:36–39
15. Tolentino-Lopez L, Segura-Cabrera A, Reyes-Loyola P, Zimic M, Quiliano M, Briz V, Muñoz-Fernández A, Rodríguez-Pérez M, Ilizaliturri-Flores I, Correa-Basurto J (2013) Biopolymers 99(1):10–21. doi:10.1002/bip.22130
16. Loyola PKR, Campos-Rodríguez R, Bello M, Rojas-Hernández S, Zimic M, Quiliano M, Briz V, Ángeles Muñoz-Fernández M, Tolentino-López L, Correa-Basurto J (2013) Immunol Res 56:44–60. doi:10.1007/s12026-013-8385-z
17. Bearman GM, Shankaran S, Elam K (2010) Drug Discov 5:152–156
18. Memoli MJ, Hrabal RJ, Hassantoufighi A, Eichelberger MC, Taubenberger JK (2010) Clin Infect Dis 50:1252–1255
19. Pizzorno A, Bouhy X, Abed Y, Boivin G (2012) Anal Chem 84(8): 3725–3730. doi:10.1021/ac300291c
20. Shie JJ, Fang JM, Lai PT, Wen WH, Wang SY, Cheng YS, Tsai KC, Yang AS, Wong CH (2011) J Am Chem Soc 133(44): 17959–17965
21. Gasymov OK, Abduragimov AR, Glasgow BJ (2012) Biochemistry 51(14):2991–3002. doi:10.1021/bi3002902
22. Frisch MJ, Trucks GW, Schlegel HB, Scuseria GE, Robb MA, Cheeseman JR, Zakrzewski VG, Montgomery JA Jr, Stratmann RE, Burant JC, Dapprich S, Millam JM, Daniels AD, Kudin KN, Strain MC, Farkas O, Tomasi J, Barone V, Cossi M, Cammi R, Mennucci B, Pomelli C, Adamo C, Clifford S, Ochterski J, Peterson GA, Ayala PY, Cui Q, Morokuma K, Malick DK, Rabuck AD, Raghavachari K, Foresman JB, Cioslowski J, Ortiz JV, Baboul AG, Stefanov BB, Liu G, Liashenko A, Piskorz P, Komaromi I, Gomperts R, Martin RL, Fox DJ, Keith T, Al-Laham MA, Peng CY, Nanayakkara A, Challacombe M, Gill PMW, Johnson B, Chen W, Wong MW, Andres JL, Gonzalez C, Head-Gordon M, Replogle ES, Pople JA (1998) Gaussian 98, Revision A.9. Gaussian, Inc., Pittsburgh
23. Morris GM, Goodsell DS, Halliday RS, Huey R, Hart E, Belew RK, Olson AJ (1998) J Comput Chem 19:1639–1662
24. Humphrey W, Dalke A, Schulten K (1996) J Mol Graph 14:33–38
25. Rayamajhi N, Joo JC, Cha SB, Pokherl S, Shin MK, Yoo YJ, Yoo HS (2011) Microbiology 11:29
26. Kanibolotsky DS, Novosyl'na OV, Abbott CM, Negrutskii BS, El'skaya AV (2008) BMC Struct Biol 8:4
27. Meijer A, Jonges M, Abbink F, Ang W, van Beek J, Beersma M, Bloembergen P, Boucher C, Claas E, Donker G, van Gageldonk-Lafeber R, Isken L, de Jong A, Kroes A, Leenders S, van der Lubben M, Mascini E, Niesters B, Oosterheert JJ, Osterhaus A, Riesmeijer R, Riezebos-Brilman A, Schutten M, Sebens F, Stelma F, Swaan C, Timen A, Van't Veen A, van der Vries E, Te Wierik M, Koopmans M (2011) Antivir Res 92(1):81–89
28.]Aoki FY, Boivin G, Roberts N (2007) Antivir Ther 12(4 Pt B):603–616
29. Storms AD, Gubareva LV, Su S, Wheeling JT, Okomo-Adhiambo M, Pan CY, Reisdorf E, St George K, Myers R, Wotton JT, Robinson S, Leader B, Thompson M, Shannon M, Klimov A, Fry AM (2012) Emerg Infect Dis 18(2):308–311. doi:10.3201/eid1802.111466
30. Kramarz P, Monnet D, Nicoll A, Yilmaz C, Ciancio B (2009) Euro Surveill 14(5):19112
31. Jardón-Valadez E, Ulloa-Aguirre A, Piñeiro A (2008) J Phys Chem B 112:10704–10713
32. Pan P, Li L, Li Y, Li D, Hou T (2013) Antivir Res 100:356–364
33. Russell RJ, Haire LF, Stevens DJ, Collins PJ, Lin YP, Blackburn GM, Hay AJ, Gamblin SJ, Skehel JJ (2006) Nature 443:45–49
34. Sine SM, Wang HL, Bren N (2002) J Biol Chem 277:29210–29223

35. Karthick V, Shanthi V, Rajasekaran R, Ramanathan K (2013) Protoplasma 250(1):197–207. doi:10.1007/s00709-012-0394-6
36. Peng DY, Sun Q, Zhu XL, Lin HY, Chen Q, Yu NX, Yang WC, Yang GF (2012) Bioorg Med Chem 20(22):6739–6750
37. Unsal-Tan O, Ozadali K, Piskin K, Balkan A (2012) Eur J Med Chem 57C:59–64
38. Yewale SB, Ganorkar SB, Baheti KG, Shelke RU (2012) Bioorg Med Chem Lett 22(21):6616–6620
39. Wang M, Qi J, Liu Y, Vavricka CJ, Wu Y, Li Q, Gao GF (2011) J Virol 85(16):8431–8435. doi:10.1128/JVI. 00638-11
40. Rudrawar S, Kerry PS, Rameix-Welti MA, Maggioni A, Dyason JC, Rose FJ, van der Werf S, Thomson RJ, Naffakh N, Russell RJ, von Itzstein M (2012) Org Biomol Chem 10(43):8628–8639